

Patient Embeddings in Healthcare and Insurance Applications

Pavel Blinov and Vladimir Kokh

Sber Artificial Intelligence Laboratory, Moscow, Russia
Blinov.P.D@sberbank.ru, Kokh.V.N@sberbank.ru

Abstract

The paper researches the problem of concept and patient representations in the medical domain. We present the patient histories from Electronic Health Records (EHRs) as temporal sequences of ICD concepts for which embeddings are learned in an unsupervised setup with a transformer-based neural network model. The model training was performed on the collection of one million patients' histories in 6 years. The predictive power of such a model is assessed in comparison with several baseline methods. A series of experiments on the MIMIC-III data show the advantage of the presented model compared to a similar system. Further, we analyze the obtained embedding space with regards to concept relations and show how knowledge from the medical domain can be successfully transferred to the practical task of insurance scoring in the form of patient embeddings.

1 Introduction

In nowadays the Electronic Health Records (EHRs) are an important and essential part of each modern national health care system, as it provides quick operations with patient-related information for all interested parties (the patient itself, an attending physician and medical staff, regulatory authorities, etc.). While a person can manually list through a single EHR data file, this task becomes tedious and labor-intensive as the number of records grows. Therefore automatic tools are required to facilitate effective interaction and comprehensive processing of EHRs.

Even more challenging problems emerge beyond simple management operations with health records. More specifically, what knowledge (and in what form?) can be extracted from a database of EHRs, and how it can be transferred to another domain? This problem is actively researched in the field of deep domain adaptation as current neural networks have a large capacity to learn transferable and useful representations between the source and target domains (Xu, He, and Shu 2020). In this paper, we address the specific problem of patient representation building within the medical domain and its application to the risk scoring task from the domain of health insurance. To find an optimal representation model, we held a series of experiments on the large industrial data feeds from both domains with hundreds

of thousands of patients spanning several years (see the Data Section 3). The main issue is that both our datasets are completely unrelated and anonymized, containing no linkage keys between each other. We present each patient from the medical dataset with a temporal sequence of their diagnosis events (defined with International Classification of Diseases codes, ICD-10 (World Health Organization 2015)) and train a neural network model to learn contextualized embeddings for each element. With such a model trained we can move all patients to an embedding space from which an averaged patient representation can be inferred. Thus we can automatically account for the medical history of insured applicants in our feature representation. Using these embeddings in our downstream insurance scoring task allows us to improve the performance metric by 1.8%.

The key contributions of this paper are the following:

- we apply the neural network model with transformer architecture to a temporal data of patient diagnosis events to build their embeddings;
- we analyze the obtained embeddings and compare them with baselines and the state-of-the-art method;
- we show that averaged patient embeddings from the medical domain can be successfully applied to the tasks from health insurance.

The rest of this paper is structured as follows. Section 2 gives an overview of related works for embeddings learning in the medical domain. The description of our datasets is given in Section 3. The modeling process and experimental results are discussed in Section 4. In the last Section 5, we provide concluding remarks and list directions of future work.

2 Related Work

To a great extent, the substantial part of the machine learning area is about finding better object representations. The current development of this problem leads to the methods of automatic feature construction (opposite to hand-crafted ones) with a neural network. Such feature vectors for modeling objects are called embeddings (Cai, Zheng, and Chang 2018). They are mainly trained in an unsupervised fashion to capture intrinsic relations between objects of a target domain, for example, word ordering and associations in natural language text.

In the medical field, the above-mentioned task is often treated as embeddings learning for the medical concepts (Choi, Chiu, and Sontag 2016; Bai et al. 2019), implying ICD diagnosis codes, terms, and abbreviations, medication and procedure names, etc. Commonly such concepts are viewed within a temporal process associated with a patient. For example, a patient has a history of clinical visits; each visit has several assigned diseases, procedures, medications, etc. In the current paper, we follow a similar modeling approach. But in favor of our practical task, we intentionally restrict the type of learnable concepts only to diagnosis codes and the most basic patient attributes (gender and age). Although this reduces the expressive power of our model but makes it language independent.

To efficiently deal with sequentially organized medical data the notion of context becomes crucial. For this, some papers (Choi, Chiu, and Sontag 2016; Bai et al. 2019) use modifications of the Skip-gram algorithm (Mikolov et al. 2013) though it is limited to account for only a fixed-size context of a sequence. Models with Recurrent Neural Network (RNN) architectures offer a better context handling mechanism. There are whole generations of RNN-based models for a patient representation task (Choi et al. 2016; Pham et al. 2016; Ma et al. 2017). We also benchmark this type of model but only as a baseline system. The bottleneck of RNNs is the single internal state vector that has to retain all information about the sequence. More advanced and powerful architectures (like current attention-based models (Vaswani et al. 2017)) can process the whole sequence context more elaborately. The model with transformer-based architecture is our central focus in this work. There are quite a few studies related to the application of transformer-like models to ICD code predictions from a variety of clinical texts (medical notes, case studies, discharge summaries, etc.) (Moons et al. 2020; Silvestri et al. 2020). In this paper, we try to abstract from atomized visits and model the entire patients’ histories to research what patterns can be learned from such patient tracks.

In this formalization, our study is most similar to (Li et al. 2020) and (Peng et al. 2020). The authors of (Li et al. 2020) use age and ICD-10 diagnosis codes from patient histories to train the Bidirectional Encoder Representations from Transformers (BERT) (Devlin et al. 2019) model and predict one of 301 patient conditions. Our primary goal was to obtain a meaningful patient representation, but the resulting model also can predict future diseases from a prefix of patient history as we train it on the Masked Language Modeling (MLM) task to predict one of 6,986 ICD-10 codes. The current paper as well as (Li et al. 2020) deals with industrial datasets of more than 1 million patients. Additionally, we compare our model performance on the open MIMIC-III (Johnson et al. 2016) dataset as in (Peng et al. 2020).

Standardization and structuring of such a complex domain as medicine is not an easy task. Unfortunately, this leads to weak compatibility between ICD versions. The transition process from the previous ICD-9 standard is still ongoing in many countries, even though the updated ICD-10 version has endorsed by the World Health Organization (WHO) in 1990. That means that many research projects and pa-

pers still had proceeded in terms of obsolete ICD-9 standards. Unlike (Choi, Chiu, and Sontag 2016; Bai et al. 2019; Peng et al. 2020) we mainly experiment with ICD-10 resorting to ICD-9 only for model comparison purposes (Section 4.2).

3 Data

At our disposal, we had three anonymized datasets: MIMIC-III (Johnson et al. 2016) and our private¹ medical (*DMed*) and insurance (*DIns*) data. We treat *DMed* as the primary data for representations learning and use *DIns* to estimate the performance of embeddings in the scoring task (see Section 4.3). Compared to our in-house datasets, MIMIC-III is rather a toy data, but it is the only open-source alternative to compare our model with the others.

In both domains, for modeling purposes, we operate on a person (patient or customer) level of abstraction. Table 1 lists summary statistics for three datasets by age decades. We pre-process the medical data closely following (Peng et al. 2020): removing infrequent ICD diagnosis codes by the threshold of 5 and leave only patients with at least two visits. For *DMed* and MIMIC-III data, the average numbers of visits are 9.9 and 2.66, respectively.

The *DIns* dataset counts 36,835,345 applicants for 8 years (from 2013 to 2020). The *DMed* data comes from a net of region-level clinics, in total including 1,063,489 patients for the 6 years (from 2014 to 2019). For the *DMed* data, we left a random 5% sample of 53,175 patients for validation and analysis. Insurance data was split by time into three parts: *train* (2013-2017), *validation* (2018), and *test* (2019 and 2020). In the insurance model development, we used *train* and *validation*, leaving the *test* for final performance estimation.

4 Medical History Modeling

In this work, we model representation of a patient’s medical history through contextualized embeddings built with transformer architecture neural network model (Devlin et al. 2019). By analogy from natural language tasks such model process sequentially organized data samples. Only a sample, instead of being a text consisting of tokens, in our case represents a patient history consisting of events in the form of ICD-10 codes. Also in general it is true that gender and age significantly affect a person’s condition and should be included in the modeling process. In our setup, we design special tokens for both genders and each age in years from 0 to 99 (see Fig. 1 for the complete sample example). In our medical dataset, we estimate the age of a patient at the moment of their last diagnosis event. In the insurance data, we know the age at the moment of an insurance application. The history lengths can significantly vary across the patients. We limit the maximum length with $H = 128$ event slots and do not remove repeating codes. By this number, we can encompass more than 99% of histories without trimming.

We try to work with only well-represented ICDs and filter out codes that encounter less than 5 times across our med-

¹Unfortunately, we cannot share this data due to legal restrictions.

Table 1: Datasets statistics.

Decade	DMed		MIMIC-III		DIns	
	Count	Male ratio, (%)	Count	Male ratio, (%)	Count	Male ratio, (%)
[0; 10)	142,549	51.8	228	52.2	19,212	48.3
[10; 20)	119,176	51.3	10	80.0	45,332	51.3
[20; 30)	183,836	49.1	181	50.8	5,522,892	46.9
[30; 40)	165,383	50.3	325	54.2	9,497,249	52
[40; 50)	127,488	50	818	57.9	8,215,431	59.4
[50; 60)	146,516	46.2	1,276	59.2	8,577,933	65.2
[60; 70)	101,071	41.9	1,613	58.5	4,603,950	63.2
[70; 80)	50,555	33.2	1,652	55.6	322,176	54.7
[80; 90)	24,265	24.1	1,393	48.4	31,170	50.2
[90; 100)	2,650	16	0	n/a	0	n/a
Total	1,063,489		7,496		36,835,345	

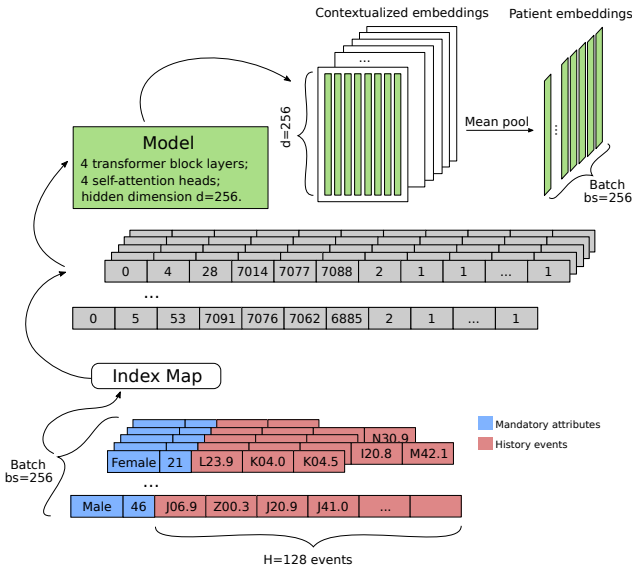


Figure 1: Scheme of data flow.

ical data. This procedure left us with 6,986 ICD-10 codes. Thus the total length of our "token" vocabulary V (with gender/age and auxiliary tokens) is $|V| = 7,096$.

Figure 1 outlines the data flow pipeline in our model. At the image bottom (in blue and red colors), a couple of history samples are presented. As the raw input samples are of different lengths, on the next step they are padded to the maximum length and converted to indices (central gray-colored part) with the *Index Map*.

As mentioned in Section 3 we use for the training 95% of patient histories (1,010,314), counting 15,522,698 ICD events. Compared to natural language data this is a rather small dataset, so we set up the following model parameters: the dimension of embedding space $d = 256$, 4 encoder layers, and 4 self-attention heads (e.g. 3 times smaller than language BERT base model (Devlin et al. 2019)). For the decoder part, the linear projection layer ($d \times |V|$) was used. Such a model was implemented with the PyTorch framework (Paszke et al. 2019) and Transformers li-

brary (Wolf et al. 2019). We trained this model on the masked token prediction task (with 25% mask probability parameter) with AdamW optimizer (learning rate of 5×10^{-5}) and batch size ($bs = 256$) of samples for 30 epochs.

At the end of training the result 256-dimensional embedding space contains points for each ICD code as well as genders and ages vectors. And a list of contextualized vectors h_1, \dots, h_k can be produced for an input sample of k -length history. To go from h_1, \dots, h_k vectors to a patient embedding h_p we resort to mean pooling operation along each of $d = 256$ dimensions over $1, \dots, k$ vectors. This is schematically depicted at the top part of Fig. 1 (green).

4.1 Embeddings analysis

To assess the quality of the trained model we performed several experiments.

First, on the medical validation set (see Section 3), we estimate the model's ability to predict the next patient's ICD code (one of 6,986) from a prefix of mandatory parameters and previous code history. We can easily do this by using the same decoder layer used for training as it returns the distribution over all V vocabulary elements from which the most probable code can be selected. By comparing actual and predicted values we compute the *Accuracy* metric (Manning, Raghavan, and Schütze 2008) for history length thresholds $th = 2..64$. There are too few validation samples after $th = 64$ to report accuracy. For example, for $th = 12$ we trim all histories at this length and drop shorter samples. Codes at the 12th position become our ground truth values and, for left samples, we predict the most probable codes from their 11 previous events.

Also for comparison purposes, we implemented three baseline algorithms: *Most common*, *Previous* and *RNN*. The *Most common* baseline always predicts the constant code of most popular disease in the train data – *J06.9 - Acute upper respiratory infection, unspecified*. The *Previous* baseline repeats the last seen value for a sample. For the *RNN* baseline we train the neural network from (Choi et al. 2016) for 30 epochs with an embedding size of 256 and 512 dimensions of gated recurrent units in two hidden layers. The performances of all algorithms are shown on *a*)-part of Fig. 2. It is

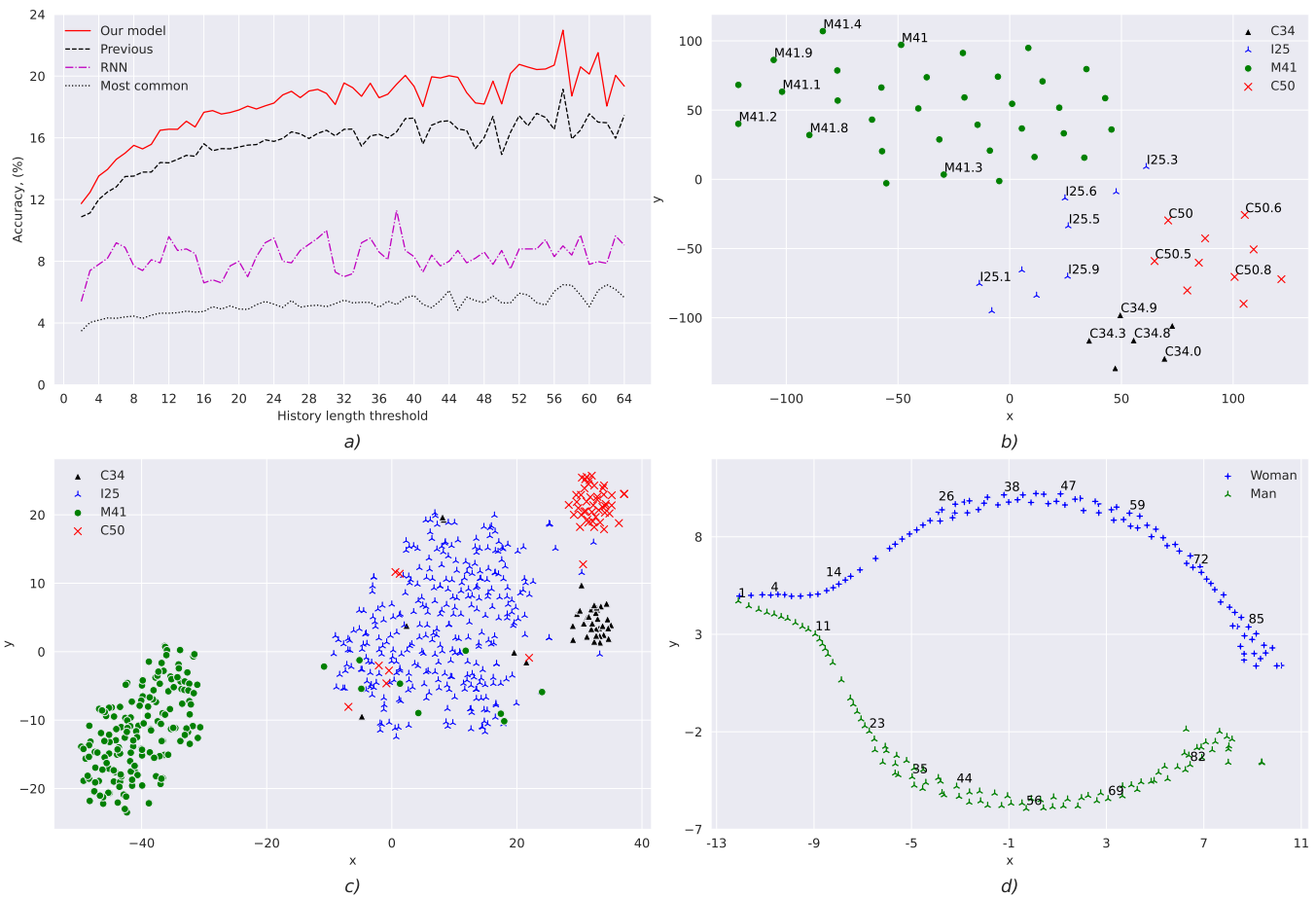


Figure 2: *a)* Model and baselines performance in next ICD code prediction task, (%); *b)* ICD code vectors from 4 disease groups (C34, M41, C50, I25); *c)* Sample of patients embeddings with C34, M41, C50 or I25 ICD codes in medical history; *d)* Averaged patient embeddings for each gender and age.

interesting to note that the *Previous* baseline shows surprisingly high performance because we keep repeating codes in histories.

Besides predictive power we want our embeddings to be interpretable, e.g. that our model learns some meaningful things, like appropriate relations between ICD codes. For example, by retrieving most similar (with cosine similarity measure (Manning, Raghavan, and Schütze 2008)) embeddings to the *J06.0*-embedding we obtain close and related diseases: *J04.2*, *J04.0*, *J20.8*, *J03.8*, or *J20.0*. As our age concepts are presented in the same embedding space we can ask ICD-age related questions, like what ages closest to the *M41.1* code? And the nearest age values would be 14, 15, 16, 12, or 11, which seems correct as the *M41.1* is *Juvenile and adolescent idiopathic scoliosis*, meaning it is the adolescent disease. Further, we can infer the risk probabilities for a specific family of diseases or even ICD-10 chapters. Fig. 3 depicts age-dependent risk curves for five disease groups. Again from this plot, one can note some reasonable dependencies learned from data like increased risk of skin disorders due to hormonal changes in a teenage body or peaking of cerebrovascular disease risks (one of the leading causes

of death globally) after the age of 50 years.

For the life and health insurance industry it is crucial to differentiate diseases by disability or mortality risk. For example, the group of *M41*-codes is definitely less risky compared to diseases in *C34*, *C50*, and *I25* code groups. We try to show this difference in our embeddings with the t-SNE (Maaten and Hinton 2008) dimensionality reduction technique. The vectors of codes from the 4 above-mentioned groups projected to 2-dimensional space are plotted at *b)*-part of Fig. 2 (for readability only some data points are labeled). More importantly, this separation seems to persist on the level of whole patient vectors. The *c)*-part of Fig. 2 plots the excerpt of 578 random patient vectors. Each patient history contains code from one of the 4 above designated groups.

Finally, we try to look at averaged patient representations, grouping patients by gender and age and presenting each group with an average of their embeddings. The result for man and woman can be seen on the *d)*-part of Fig. 2. Each point on the plot is an averaged representation of thousands of patients. Again we labeled with age value only several data points. It is interesting to see clear gender separation

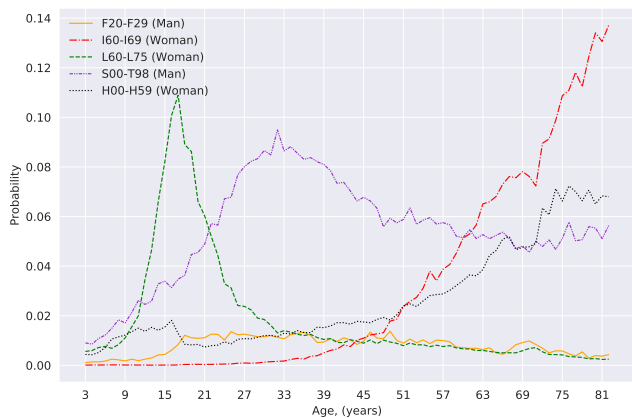


Figure 3: Risk curves for: *F20-F29* (Schizophrenia, schizotypal and delusional disorders); *I60-I69* (Cerebrovascular diseases); *L60-L75* (Disorders of skin appendages); *S00-T98* (Injury, poisoning and certain other consequences of external causes); *H00-H59* (Diseases of the eye and adnexa).

and some age tendencies.

Here it is worth noting that the axis on *b)-d)* plots of Fig. 2 do not have any physical meaning. And we cannot draw precise conclusions just from these plots as the t-SNE algorithm only tries to approximate relative object positions on the plain as close to their positions in the original high dimensional space. By these plots, we intended to provide only a general overview of the resulting embedding space and hope that it can adequately represent the medical concepts and patients.

4.2 MIMIC-III benchmark

Moreover, we compare our model to available state-of-the-art methods. Many medical models (Song et al. 2018; Qiao et al. 2019; Peng et al. 2020) benchmark their performance on the open-source MIMIC-III (Johnson et al. 2016) dataset in the typical task of next diagnosis prediction. This dataset uses ICD-9 diagnosis coding scheme. As mentioned in Section 2 there is weak compatibility between ICD-10 and ICD-9 standards. So we cannot directly apply our model and had to retrain it with these data and slight modifications in the architecture².

Predictions in the MIMIC-III benchmark often have to be made not for disease codes themselves but categories in their hierarchical grouping (Choi et al. 2016; Peng et al. 2020), e.g. some form of medical risks. Following this tradition, we use second-level categories of the Clinical Classifications Software³ as possible model outcomes. This procedure reduces output space from thousands of codes to 136 categories.

The common metric to evaluate models in such a setting is *Precision at k*, which measures the percentage of relevant

categories in the retrieved result of length k :

$$Precision@k = \frac{|top_k \cap \hat{y}|}{\min(k, |\hat{y}|)},$$

where top_k is the set of predicted categories, \hat{y} is the set of actual categories in the next patient visit.

Given the small data size instead of a single validation split, we perform a 10-fold cross-validation procedure (Bishop 2006) to estimate the mean and standard deviation of *Precision@k* for $k = [5, 10, 20, 30]$ values. Table 2 shows the results for several variants of our model. Also as a reference, we include the result of *MusaNet* from (Peng et al. 2020), which claims to be state-of-the-art in this dataset and task.

The default choice in transformer-like models is the use of special classification (CLS) token representation (Devlin et al. 2019) as the summary representation of a whole sample. But in this task such version of the model (*v.CLS*) is actually performing poorly. The *MusaNet*'s result is overcome by using more advanced pooling strategies over contextualized embeddings proposed in (Blinov et al. 2020). Such a model (*v.cmm_wo_gender/age*) achieves comparable results (given the standard deviation) even without gender and age embeddings. And the model (*v.cmm*) utilizing this piece of data outperforms the *MusaNet*. We also found that the transformer model without the positional embedding layer (*v.cmm_wo_positional*) performs slightly better. From this, we can conclude that in the risk prediction task the composition of patient diseases is more important than their specific ordering. Overall, the above experiments confirm that transformer models allow building the state-of-the-art system for the prediction of subsequent patient risks.

4.3 Insurance scoring

We apply the above-discussed model in one of our current projects. The stakeholders from an insurance company want to rebuild and automate part of their scoring pipeline. Insurance risk can vary widely for different customers depending on many factors. An accurate predictive model for risk assessment leads to an optimal personalized charge which is beneficial for a company and customer. The core modeling object in such a problem is an *Application for insurance Policy, AP*. Formally it requires to build a model f which for a given AP predicts the risk value r : $f(AP) = r$. The risk r defined as the following: claim of insurance sum during the first year period, e.g. it is a binary event - whether an AP resulted in a loss. Therefore it was decided to address the problem as a binary classification task.

At our disposal, we had the dataset of historical AP s for several years (see Section 3). From these data it was concluded that each AP object consists of two major parts: *Applicant, A* and *Policy, P*. The A -part contains person-related features such as gender, age, diseases anamnesis in the form of free text and ICD-10 codes. The P -part includes all contract-related features (insurance period and product type, insured sum and currency, region, etc.). Also according to historical $DIns$ data the binary target is very skewed with less than 1% of claims.

²This code is available at <https://github.com/sberbank-ai-lab/mimic.profile>

³<https://www.hcup-us.ahrq.gov/toolssoftware/ccs/ccs.jsp>

Table 2: Systems performances in next diagnoses prediction task, (%).

System	Precision@k			
	k=5	k=10	k=20	k=30
MusaNet (Peng et al. 2020)	65.07	60.69	71.04	82.27
v.CLS	61.92±1.11	57.3±1.03	67.77±0.79	77.99±0.72
v.cmm_wo_gender/age	65.86±0.94	60.98±0.6	71.7±0.36	81.3±0.6
v.cmm	66.41±0.99	61.62±0.87	72.07±0.64	81.83±0.45
v.cmm_wo_positional	66.77±0.84	61.9±0.99	72.58±0.83	82.17±0.45

Table 3: Validation ROC AUC metrics of the scoring model, (%).

Scheme	Month												Average
	1	2	3	4	5	6	7	8	9	10	11	12	
Base	71.6	72.4	71.9	70.4	67.1	71.7	70.4	72.5	71.2	69.5	71.8	69.4	70.83
Replacement	75	74.1	73.6	72.6	69.1	72.2	71.8	74	72.8	71.6	73.6	71.6	72.65

Given *AP* features separation we can use patient embeddings to fully represent the whole *A*-part in a unified fashion. Accounting on the properties of our embedding space we can naturally process applicants with rare or even unseen disease anamnesis. For instance, there are many applicants with the *I25* disease and mostly they are in the high-risk group. Suppose in a new *AP* we encountered with the *I21* diagnosis code unseen in *DIns* data. But both *I25* and *I21* relate to heart disease and their vectors are close together in the embedding space (as we learned from medical data) so we can more precisely assess the risk in this case.

It is worth noting that due to the early stage of this project development substantial part of diagnosis-related features is still in the process of consolidation. In the case of an empty anamnesis feature field, we use just averaged (by gender and age) patient representations. Also, the important requirement to the model was the stability of predictions in time and interpretability. For these reasons, we choose a Ridge model as above mentioned *f* function. This model is compared under two schemes: *Base* and *Replacement*. In the *Base* scheme only insurance data were used. *A*-part features were one hot encoded before concatenation to *P*-features. In the *Replacement* scheme the *A*-part features group was replaced by 256-dimensional patient embeddings. The model’s performance was measured by the ROC AUC metric (Manning, Raghavan, and Schütze 2008). Table 3 shows the average and by-month metric values under both schemes for the validation year. It can be seen that both models are stable by months. The *Replacement* scheme yields solid metric improvements ranging from 0.5% to 3.4% and 1.82% in the year average. This allows us to conclude that using patient embeddings helps in the given task. We hope to further improve the metric as the full insurance features become available.

Model deployment. To integrate the developed model in the current scoring pipeline, we prototyped RESTful web service using Flask framework. The service receives an applicant data from insurance software, run the transformer neural network to get an applicant embedding, apply the final Ridge model *f(AP)* and return the result. As we plan to

assess this model performance through A/B testing the service also logs each query in the Postgres database for further analytical purposes.

When designing a service for a real-time use case scenario, the response time is a primary consideration. In the above-listed steps, the most time-consuming one is the transformer-model inference. It depends on the computation device specification, for instance with NVIDIA Tesla V100 GPU it takes on average 6.6 ms to process a single query. The CPU version is roughly ten times slower - 68.6 ms per request, but for the pilot period, even this performance is enough to manage our current workload. For smooth deployment, we packed the whole service into a docker image, separating it from the database. In such a way, the application allows horizontal scaling under increasing load by running more processing containers that share a single database located in another container.

Another concern to address is the stability monitoring of the hosted model. For this, we selected Population Stability Index (PSI) (Siddiqi 2012), which measures the difference between model score distributions on development and production sets. Weekly basis tracking of the PSI allows quickly detect an unexpected model behavior to reduce financial and time loss.

5 Conclusions

We presented the way of working with medical data on the level of holistic patient histories through embedding space built with the neural network with transformer architecture. Model analysis revealed that it automatically learns several plausible medical patterns and adequately preserves relation between concepts. Potentially, the model has several practical applications, for example, it can be used as an EHR indexing tool for retrieval purposes, analysis, and discovery of patients with chronic diseases, etc.

Our experiments on the MIMIC-III data showed that the inclusion of gender and age-specific information without positional embeddings allows us to achieve the new state-of-the-art result in the next diagnosis prediction task. We release the code of that experiment, hoping it’ll be useful for other EHR-related researches. Next, we’ll plan to extend the

described representation approach by trying to incorporate more medical concepts in the model.

Finally, we showed how patient representation could be extracted from the embedding space and successfully applied to the task from the related insurance domain. On the validation data, we obtained the stable ROC AUC metric improvement of 1.82%. To finally verify benefits of this model we plan to pilot it in the production environment. At our point of view the deployment of such model has couple of major challenges for both of which we propose reasonable solutions.

Acknowledgements

We are grateful to Alexander Nesterov for his assistance with MIMIC-III data access.

References

- Bai, T.; Egleston, B. L.; Bleicher, R.; and Vucetic, S. 2019. Medical Concept Representation Learning from Multi-source Data. In *IJCAI*, 4897–4903.
- Bishop, C. M. 2006. *Pattern recognition and machine learning*. Springer.
- Blinov, P.; Avetisian, M.; Kokh, V.; Umerenkov, D.; and Tuzhilin, A. 2020. Predicting Clinical Diagnosis from Patients Electronic Health Records Using BERT-based Neural Networks. In *International Conference on Artificial Intelligence in Medicine*, 111–121. Springer.
- Cai, H.; Zheng, V. W.; and Chang, K. C.-C. 2018. A comprehensive survey of graph embedding: Problems, techniques, and applications. *IEEE Transactions on Knowledge and Data Engineering*, 30(9): 1616–1637.
- Choi, E.; Bahadori, M. T.; Schuetz, A.; Stewart, W. F.; and Sun, J. 2016. Doctor ai: Predicting clinical events via recurrent neural networks. In *Machine learning for healthcare conference*, 301–318. PMLR.
- Choi, Y.; Chiu, C. Y.; and Sontag, D. A. 2016. Learning Low-Dimensional Representations of Medical Concepts. In *Summit on Clinical Research Informatics, CRI 2016, San Francisco, CA, USA, March 21-24, 2016*. AMIA.
- Devlin, J.; Chang, M.-W.; Lee, K.; and Toutanova, K. 2019. BERT: Pre-training of Deep Bidirectional Transformers for Language Understanding. arXiv:1810.04805.
- Johnson, A. E.; Pollard, T. J.; Shen, L.; Li-Wei, H. L.; Feng, M.; Ghassemi, M.; Moody, B.; Szolovits, P.; Celi, L. A.; and Mark, R. G. 2016. MIMIC-III, a freely accessible critical care database. *Scientific data*, 3(1): 1–9.
- Li, Y.; Rao, S.; Solares, J. R. A.; Hassaine, A.; Ramakrishnan, R.; Canoy, D.; Zhu, Y.; Rahimi, K.; and Salimi-Khorshidi, G. 2020. BeHRt: transformer for electronic Health Records. *Scientific Reports*, 10(1): 1–12.
- Ma, F.; Chitta, R.; Zhou, J.; You, Q.; Sun, T.; and Gao, J. 2017. Dipole: Diagnosis prediction in healthcare via attention-based bidirectional recurrent neural networks. In *Proceedings of the 23rd ACM SIGKDD international conference on knowledge discovery and data mining*, 1903–1911.
- Maaten, L. v. d.; and Hinton, G. 2008. Visualizing data using t-SNE. *Journal of machine learning research*, 9(Nov): 2579–2605.
- Manning, C. D.; Raghavan, P.; and Schütze, H. 2008. *Introduction to Information Retrieval*. USA: Cambridge University Press. ISBN 0521865719.
- Mikolov, T.; Chen, K.; Corrado, G.; and Dean, J. 2013. Efficient estimation of word representations in vector space. *arXiv preprint arXiv:1301.3781*.
- Moons, E.; Khanna, A.; Akkasi, A.; and Moens, M.-F. 2020. A comparison of deep learning methods for ICD coding of clinical records. *Applied Sciences*, 10(15): 5262.
- Paszke, A.; Gross, S.; Massa, F.; Lerer, A.; Bradbury, J.; Chanan, G.; Killeen, T.; Lin, Z.; Gimelshein, N.; Antiga, L.; Desmaison, A.; Köpf, A.; Yang, E.; DeVito, Z.; Raison, M.; Tejani, A.; Chilamkurthy, S.; Steiner, B.; Fang, L.; Bai, J.; and Chintala, S. 2019. PyTorch: An Imperative Style, High-Performance Deep Learning Library. arXiv:1912.01703.
- Peng, X.; Long, G.; Shen, T.; Wang, S.; and Jiang, J. 2020. Self-attention Enhanced Patient Journey Understanding in Healthcare System. In Hutter, F.; Kersting, K.; Lijffijt, J.; and Valera, I., eds., *Machine Learning and Knowledge Discovery in Databases - European Conference, ECML PKDD 2020, Ghent, Belgium, September 14-18, 2020, Proceedings, Part III*, volume 12459 of *Lecture Notes in Computer Science*, 719–735. Springer.
- Pham, T.; Tran, T.; Phung, D.; and Venkatesh, S. 2016. Deepcare: A deep dynamic memory model for predictive medicine. In *Pacific-Asia conference on knowledge discovery and data mining*, 30–41. Springer.
- Qiao, Z.; Wu, X.; Ge, S.; and Fan, W. 2019. MNN: multi-modal attentional neural networks for diagnosis prediction. *Extraction*, 1: A1.
- Siddiqi, N. 2012. *Credit risk scorecards: developing and implementing intelligent credit scoring*, volume 3. John Wiley & Sons.
- Silvestri, S.; Gargiulo, F.; Ciampi, M.; and De Pietro, G. 2020. Exploit Multilingual Language Model at Scale for ICD-10 Clinical Text Classification. In *2020 IEEE Symposium on Computers and Communications (ISCC)*, 1–7.
- Song, H.; Rajan, D.; Thiagarajan, J.; and Spanias, A. 2018. Attend and diagnose: Clinical time series analysis using attention models. In *Proceedings of the AAAI Conference on Artificial Intelligence*, volume 32.
- Vaswani, A.; Shazeer, N.; Parmar, N.; Uszkoreit, J.; Jones, L.; Gomez, A. N.; Kaiser, Ł.; and Polosukhin, I. 2017. Attention is all you need. In *Advances in neural information processing systems*, 5998–6008.
- Wolf, T.; Debut, L.; Sanh, V.; Chaumond, J.; Delangue, C.; Moi, A.; Cistac, P.; Rault, T.; Louf, R.; Funtowicz, M.; Davison, J.; Shleifer, S.; von Platen, P.; Ma, C.; Jernite, Y.; Plu, J.; Xu, C.; Scao, T. L.; Gugger, S.; Drame, M.; Lhoest, Q.; and Rush, A. M. 2019. HuggingFace’s Transformers: State-of-the-art Natural Language Processing. arXiv:1910.03771.
- World Health Organization. 2015. *International statistical classification of diseases and related health problems*.

World Health Organization, 10th revision, fifth edition, 2016 edition.

Xu, W.; He, J.; and Shu, Y. 2020. Transfer Learning and Deep Domain Adaptation. In *Advances in Deep Learning*. IntechOpen.